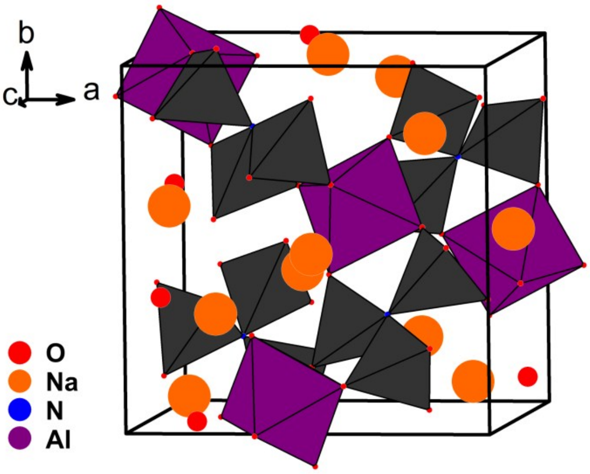

S1: Crystal structure of cubic $Na_3AlP_3O_9N$, $P(O,N)_4$ tetrahedra in gray and AlO_6 octahedra highlighted in violet.[1,2]

S2: Synthesis of $AlP_6O_{3x}(NH)_{3-3x}N_9$ ($x \approx 0.33$): Al powder (7.3 mg, 0.27 mmol, Grüssing, 99.99% metal content), amorphous HPN_2 (97.2 mg, 1.62 mmol, synthesized according to Lücke, ref. 3), $HgCl_2$ (0.7 mg, 1 mol% in relation to Al; as activator, i.e. for the amalgamation of Al) and NH_4Cl (1.0 mg, 1 mol% in relation to Al; as mineralizer) were ground in a ball mill (Specamill GS06000 with agate capsule and agate balls, Specac) with 2 balls (3 x 3 min). Oxygen impurities in starting materials could not be excluded completely. The mixture was tightly packed in a crucible of hexagonal boron nitride (Henze, Kempten) and closed with a cap of the same material. The reaction was carried out in a Walker-type multianvil assembly as described in ref. 4 and 5. The material was compressed to 5 GPa at room temperature and then heated to 1100 °C in 30 minutes. This temperature was held for 60 minutes and then cooled down in 120 minutes. After slow decompression (12 h), $AlP_6O_{3x}(NH)_{3-3x}N_9$ ($x \approx 0.33$) was obtained as a microcrystalline gray powder, stable against air and moisture.

S3: Electron Microscopy: Scanning electron microscopy (SEM) was done with a Jeol JSM 6500F (Jeol, Germany) equipped with energy dispersive X-ray (EDX) detector (model 7418, Oxford Instruments, Great Britain). The sample was fixed on electrically conductive tabs (G3347, Plano GmbH, Germany). For transmission electron microscopy (TEM), microcrystals of $AlP_6O_{3x}(NH)_{3-3x}N_9$ were ground in absolute ethanol and drop-cast on copper finder grids with a continuous carbon film (S160NH2, Plano GmbH, Germany) before transferring them into the TEM on a double-tilt holder. A Jeol 2010 (Jeol, Germany) with a LaB_6 emitter operated at 200 kV acceleration voltage combined with a TEMCam F216 camera (TVIPS, Germany, resolution 2k x 2k) and an EDAX Apollo XLT EDX detector (EDAX, Germany) was used for preliminary studies. In addition, a Titan 80-300 (FEI, USA) with a field emitter operated at 300 kV or 120 kV acceleration voltage combined with an UltraScan 1000 Camera (Gatan, USA, resolution 2k x 2k) and a TEM TOPS 30 EDX spectrometer (Gatan, Germany) was used. Electron energy loss spectroscopy (EELS) was done on the Titan 80-300 in STEM mode at 300 kV acceleration voltage with a post-column filter (GIF Tridiem 893, Gatan, Germany). For EELS measurements, the sample was plasma-cleaned for 20 s. The product is moderately electron-beam sensitive at acceleration voltages of 120-300 kV. For the evaluation of the TEM data, the following software was used: Digital Micrograph (EELS spectra), ProcessDiffraction7 (geometric calculations for selected area electron diffraction, SAED) and JEMS (SAED simulations), ES Vision and EDAX TEAM (EDX spectra).[6-7]

S4: Synchrotron Measurements and Crystal Structure Analysis: All single-crystal experiments were done at beamline ID11 of the ESRF (Grenoble, France) at a wavelength of 0.3351 Å (Si(111) double-crystal monochromator). The TEM grid containing the precharacterized microcrystals was fixed on a glass fiber on a goniometer head. The alignment of the crystal in the focused X-ray beam (ca. 4 x 6 µm) was done by an optical telescope, followed by more accurate centering via collecting single diffraction patterns while slightly shifting the sample. The data was recorded using a Frelon2k CCD detector and indexed as well as integrated with Crysalis.[8] Parasitic scattering from Cu TEM grid was discarded. Further correction of the incident-angle-dependent detector absorption [9] and scaling as well as semi-empirical absorption correction was done.[11] Further details on the structure analysis can be obtained from the Fachinformationszentrum Karlsruhe, 76344 Eggenstein-Leopoldshafen, Germany (fax: +49-7247-808-666; e-Mail: crysdata@fiz-karlsruhe.de) on quoting the depository number CSD-431557.

S5: Powder X-Ray Diffraction: Powder diffraction patterns (samples filled in 0.3 mm in diameter glass capillaries under Ar; for temperature dependant measurements quartz glass capillaries of 0.3 mm in diameter were used) were collected at room temperature with a Stoe StadiP (Cu $K_{\alpha 1}$ radiation, modified Debye-Scherrer geometry, Ge(111) monochromator) and a Mythen 1K silicon stripe detector. Temperature dependant powder diffraction patterns were collected with a Stoe StadiP (Mo $K_{\alpha 1}$ radiation, modified Debye-Scherrer geometry, Ge(111) monochromator) and a Mythen 1K silicon stripe detector in 20 K steps to a maximum of 1000 °C. Data were collected at constant temperature. Rietveld refinements were done with Topas Academic [10] employing the fundamental parameters approach [11,12] and using spherical harmonics of fourth order for modeling preferred orientation.[13]

S6: FTIR spectroscopy: The FTIR spectra of $AlP_6O_{3x}(NH)_{3-3x}N_9$ ($x \approx 0.33$) were recorded with a Perkin-Elmer Spectrum BX II spectrometer using KBr pellets. The FTIR spectrum shows weak and broad absorption bands in the range from 3250 - 2600 cm^{-1} corresponding to N-H valence modes. The strong absorption bands between 1500 and 800 cm^{-1} are characteristic for (imidooxo)nitridophosphate networks.[14-15]

S7: Solid-state nuclear magnetic resonance (NMR) spectroscopy: Solid-state NMR spectra were acquired on a Bruker Avance-III spectrometer with an 11.7 T magnet, operating at a ^1H frequency of 500.25 MHz, using a commercial 1.3 mm double-resonance MAS probe. For all measurements, the ^1H resonance of 1% $Si(CH_3)_4$ in $CDCl_3$ was used as an external secondary reference.

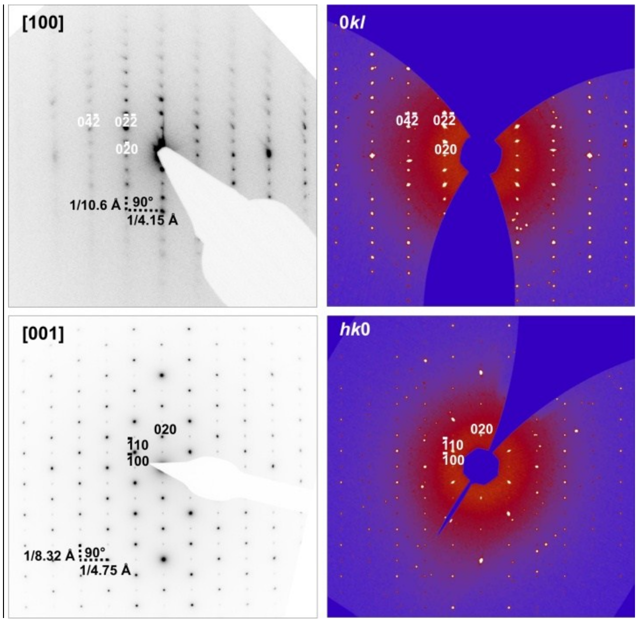

S8: SAED patterns (300 kV) from different crystallites (left, including directly measured unit cell parameters) compared to reciprocal lattice sections reconstructed from single crystal X-ray diffraction data (right).

The comparison between reciprocal lattice sections reconstructed from single-crystal X-ray diffraction data and SAED patterns in accordance to the monoclinic metrics. Neither in SAED patterns (S10, left) nor in the reciprocal lattice sections (S10, right) there is additional intensity between reflections along [001]. This would be expected for an enlargement of the unit cell regarding the related compounds $MH_4P_6N_{12}$ with M = Ca, Mg.

S9: TEM EDX measurements (300 kV) of $AlP_6O_{3x}(NH)_{3-3x}N_9$ in atom% (standard deviation).

	Al (K)	**P (K)**	**N (K)**	**O (K)**
K1	5.7	29.2	60.2	4.8
K2	6.0	32.8	58.3	2.9
K3	6.5	34.6	56.2	2.7
K4	5.6	30.7	56.9	6.8
K5	5.4	34.1	57.9	2.5
K6	6.4	34.7	56.6	2.3
K7	6.2	33.0	53.7	7.2
K8	6.0	35.2	52.5	5.7
K9	6.2	34.6	53.0	6.2
mean value	**6.1(4)**	**33.2(20)**	**56.1(26)**	**4.6(20)**
ideal value	**5.3**	**31.6**	**57.9**	**5.3**

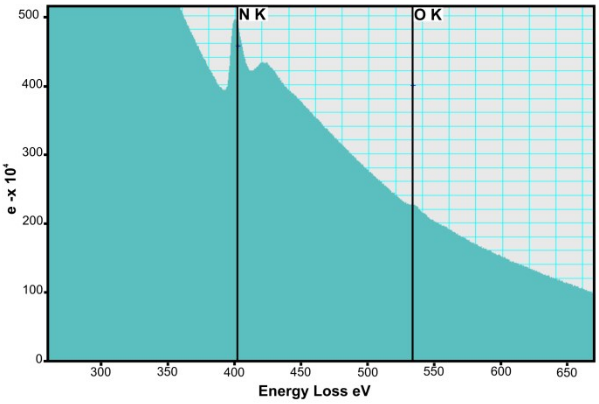

S10: EELS spectrum (300 kV) of $AlP_6O_{3x}(NH)_{3-3x}N_9$, black lines represent positions of N-K and O-K edges.

The EELS spectrum shows the N-K edge at 401 eV energy loss as well as the O-K edge at 532 eV energy loss. The ratio of N:O based on EELS measurements is with 9:1 close to the ratio of 11:1 for $AlP_6O_{3x}(NH)_{3-3x}N_9$.

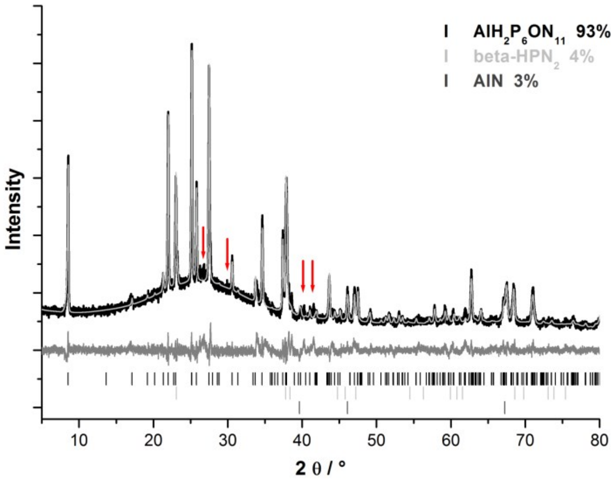

S11: Rietveld refinement of $AlP_6O_{3x}(NH)_{3-3x}N_9$, observed (thick black line) and calculated (thin light gray line) powder diffraction patterns as well as difference plot (dark gray line) and positions of Bragg reflections (black: $AlP_6O_{3x}(NH)_{3-3x}N_9$, light gray: β-$HPN_2$, dark grey: AlN).

Additional unexplained reflections (red arrows in Fig. S11) belong to an unknown side phase. The structure determination of that side phase was not possible because no matching crystals for the combination of TEM and microfocused synchrotron diffraction could be found. The lattice parameters of $AlP_6O_{3x}(NH)_{3-3x}N_9$ obtained by the Rietveld refinement show a small deviation (volume difference of 0.9 %) from those obtained by single-crystal measurements. This is probably caused by chemical variations in $AlP_6O_{3x}(NH)_{3-3x}N_9$, represented by x.

S12: Crystallographic data of Rietveld refinement of $AlP_6O_{3x}(NH)_{3-3x}N_9$ with x ≈ 0.33 and with standard deviation in parentheses.

	$AlH_2P_6ON_{11}$	beta-HPN_2	AlN
molar weight (in g/mol)	384.892	33.116	40.988
space group (no.)	$P2_1/m$ (11)	$\bar{4}2d$ (122)	$Fm\bar{3}m$ (225)
unit cell parameters (in Å / °)	a = 4.7416(2) b = 8.3250(3) c = 10.623(6) β = 102.88(1)	a = 4.749(5) c = 6.55(1)	a = 3.9373(4)
cell volume (in Å^3)	408.79(4)	147.9(4)	61.03(2)
x-ray density (in g/cm^3)	3.1271(3)	2.694(7)	4.461(1)
absorption µ (in mm^{-1})	13.611(1)	11.48(3)	15.748(5)
number of reflections	277	17	3
spherical harmonics	4	0	0
R_{Bragg}	0.0348	0.0391	0.0667
independent parameters		53	
background parameters		18	
R_p / R_{wp}		0.0601 / 0.0797	
GooF		1.570	

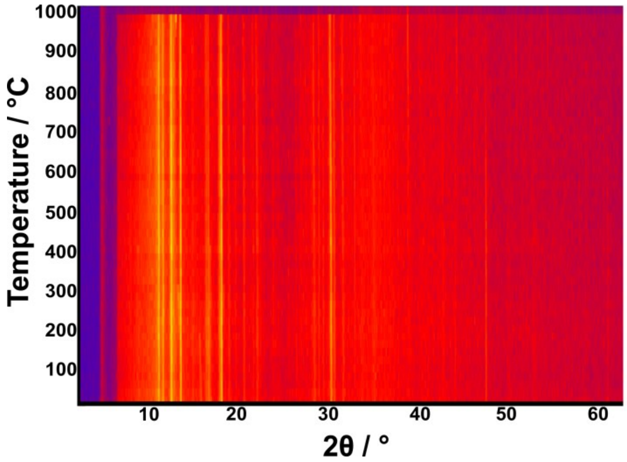

S13: Temperature-dependant X-ray powder diffraction pattern of $AlP_6O_{3x}(NH)_{3-3x}N_9$.

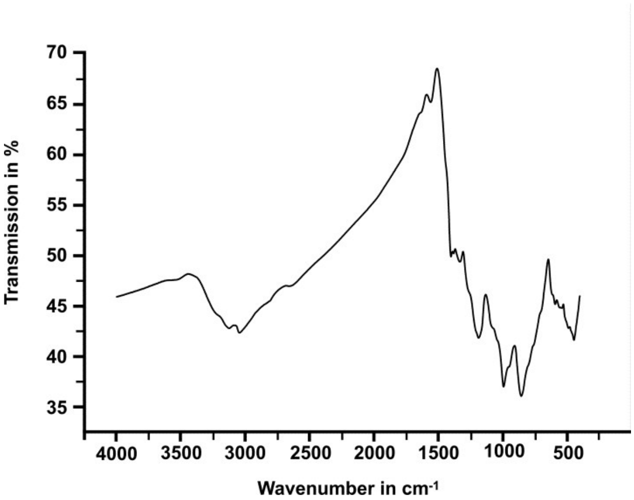

S14: FTIR spectrum of $AlP_6O_{3x}(NH)_{3-3x}N_9$.

S15: Crystallographic data and details of the structure refinement of $AlP_6O_{3x}(NH)_{3-3x}N_9$ with $x \approx 0.33$ and with standard deviation in parentheses.

formula	$AlP_6O(NH)_2N_9$
molar weight (in g/mol)	384.892
crystal system / space group (no.)	monoclinic / $P2_1/m$ (no. 11)
lattice parameters (in Å, °)	a = 4.7566(2), b = 8.3266(3), c = 10.6298(7),
	β = 101.601(4)
cell volume (in Å^3)	412.41(4)
density (in g·cm^{-3})	3.100
formula units per unit cell	2
F(000)	380
θ range (in °)	$2.061 \leq \vartheta \leq 13.846$
wavelength (in Å)	0.3351
total no. of reflections / independent reflections	1285 / 1103
refined parameters / restraints	105 / 0
R-values(all data)	$R1 = 0.0351$, $wR2 = 0.0735$
R-values ($F^2 > 2\sigma(F^2)$)	$R1 = 0.0285$, $wR2 = 0.0702$
goodness of fit	1.046
absorption coefficient (in mm^{-1})	0.196
weight	$w = 1/ [\sigma^2(F_0^2) + (0.0205P)^2+0.1217P]$*
$\Delta\rho_{max}$, $\Delta\rho_{min}$ (in e Å^{-3})	+0.63, -0.51

* $P = [2F_c^2 + Max(F_0^2,0)]/3$

S16: Atom coordinates and equivalent isotropic displacement parameters (in Å^2) of $AlP_6O_{3x}(NH)_{3-3x}N_9$ with standard deviation in parentheses.

atom	Wyckoff site	*x*	*y*	*z*	U_{eq}	s. o. f.
P1	4*f*	0.16554(8)	0.08551(4)	0.32927(5)	0.00890(12)	1
P2	4*f*	0.33412(8)	0.08486(4)	0.67156(5)	0.00893(12)	1
P3	2*e*	0.10774(12)	1/4	0.08409(7)	0.01196(14)	1
P4	2*e*	0.53473(12)	1/4	0.91759(7)	0.01218(15)	1
Al5	2*e*	0.75102(12)	1/4	0.50031(7)	0.00978(16)	1
N1/O1	2*e*	0.4273(4)	1/4	0.0511(2)	0.0218(5)	0.48(3)/0.52(3)
N2/O2	2*e*	0.8816(4)	1/4	0.9501(2)	0.0225(5)	0.52(3)/0.48(3)
N3	4*f*	0.0177(3)	0.57434(15)	0.37888(16)	0.0098(3)	1
N4	4*f*	0.5186(3)	0.07479(15)	0.37899(16)	0.0100(3)	1
N5	4*f*	0.0718(3)	0.09399(16)	0.17310(17)	0.0119(3)	1
N6	4*f*	0.5837(3)	0.59393(16)	0.17146(17)	0.0126(3)	1
N7	2*e*	0.0518(4)	1/4	0.3889(2)	0.0093(3)	1
N8	2*e*	0.4556(4)	1/4	0.6163(2)	0.0094(4)	1
H5	4*f*	0.02(2)	0.029(15)	0.129(15)	0.11(3)*	0.5
H6	4*f*	0.60(2)	0.517(17)	0.126(14)	0.11(3)*	0.5

* For both H atoms the same displacement parameter was used.

S17: Anisotropic displacement parameters (in Å^2) of $AlP_6O_{3x}(NH)_{3-3x}N_9$ with standard deviation in parentheses.

Atom	U_{11}	U_{22}	U_{33}	U_{12}	U_{13}	U_{23}
P1	0.00643(18)	0.00652(19)	0.0141(3)	-0.00008(13)	0.00287(14)	-0.00016(11)
P2	0.00664(19)	0.00627(19)	0.0142(3)	0.00001(13)	0.00288(14)	-0.00004(11)
P3	0.0097(2)	0.0133(3)	0.0132(3)	0	0.00299(19)	0
P4	0.0102(2)	0.0123(3)	0.0139(3)	0	0.0021(2)	0
AL5	0.0083(3)	0.0089(3)	0.0128(4)	0	0.0036(3)	0
N1/O1	0.0118(8)	0.0343(12)	0.0200(13)	0	0.0049(7)	0
N2/O2	0.0125(8)	0.0361(12)	0.0189(13)	0	0.0031(7)	0
N3	0.0071(5)	0.0079(5)	0.0146(8)	-0.0011(5)	0.0023(5)	0.0002(4)
N4	0.0072(5)	0.0075(5)	0.0152(8)	-0.0010(5)	0.0023(5)	0.0003(4)
N5	0.0122(6)	0.0098(6)	0.0137(8)	-0.0002(5)	0.0026(5)	-0.0010(4)
N6	0.0149(6)	0.0103(6)	0.0122(8)	0.0000(5)	0.0016(5)	0.0020(5)
N7	0.0078(7)	0.0069(7)	0.0137(11)	0	0.0036(6)	0
N8	0.0080(7)	0.0071(7)	0.0134(11)	0	0.0033(6)	0

S18: Bond lengths in $AlP_6O_{3x}(NH)_{3-3x}N_9$ with standard deviation in parentheses.

bond	length (in Å)	bond	length (in Å)
P1-N3	1.6413(14)	P3-N5	1.6361(15)
P1-N4	1.6585(15)	P4-N1/O1	1.6022(24)
P1-N5	1.6315(18)	P4-N2/O2	1.6164(21)
P1-N7	1.6454(11)	P4-N6	1.6394(16)
P2-N3	1.6535(15)	Al5-N3	2.1050(15)
P2-N4	1.6426(14)	Al5-N4	2.1071(15)
P2-N6	1.6373(18)	Al5-N7	2.0329(20)
P2-N8	1.6453(11)	Al5-N8	2.0470(20)
P3-N1/O1	1.6273(19)	N5-H5	0.73(14)
P3-N2/O2	1.6030(25)	N6-H6	0.81(15)

Taking only X-ray data into account, the assignment of light-atom sites in $AlP_6O_{3x}(NH)_{3-3x}N_9$ is not unequivocal. Miscellaneous refinements with small differences in the occupancy of the light atoms yielded various models of the occupancy of H, N and O sites in the zig-zag tetrahedra chains but showed not significant differences in their figures of merit (*R*-values, GooF, interatomic distances, residual electron density). H positions are assigned to residual electron density and NMR investigations, N-H bond lengths refined. Bond-valence sum calculations[16] were considered and the final model yielded suitable values for all cations (difference of P^{5+} and Al^{3+} < 7%) and helped with the assignment of N vs. O/NH on the anion sites. The result is that Al is surrounded only by N atoms (N3, N4, N7, N8; difference < 5%). Both N-H groups and N/O mixed occupied sites are located in the zig-zag chains because the N1/N2 BVS values for only N on this sites were too small (up to 11%) and the corresponding O1/O2 values for only O were too high (up to 24%). In the final refinement, the compositely occupied positions N1/O1 and N2/O2 showed the same ratio of O and N.

---

1 J. Ronis, B. Y. Bondars, A. A. Vitola, T. Miller, *Latv. Kim. Z.*, 1993, **1**, 662.

2 R. Conanec, P. L´Haridon, W. Feldmann, R. Marchand, Y. Laurent, *Eur. J. Solid State Inorg. Chem.*, 1994, **31**, 13.

3 W. Schnick, J. Lücke, *Z. Anorg. Allg. Chem.*, 1992, **610**, 121.

4 a) N. Kawai, S. Endo, *Rev. Sci. Instrum.,* 1970, **41**, 1178; b) D. Walker, M. A. Carpenter, C. M. Hitch, *Am. Mineral.,* 1990, **75**, 1020; c) D. Walker, *Am. Mineral.,* 1991, **76**, 1092; d) D. C. Rubie, *Phase Transitions,* 1999, **68**, 431; e) H. Huppertz, *Z. Kristallogr.*, 2004, **219**, 330.

5 A. Marchuk, L. Neudert, O. Oeckler, W. Schnick, *Eur. J. Inorg. Chem.,* 2014, **21**, 3427.

6 Digital Micrograph, *version 3.6.1*, *Gatan Software Team*, USA, 1999.

7 TEAM, version *3.4.1, EDAX AMETEK*, Wiesbaden, Germany, 2013.

8 CrysAlisPro 1.171.38.41, Rigaku Oxford Diffraction, Great Britain, 2015.

9 G. Wu, B. L. Rodrigues, P. Coppens, *J. Appl. Crystallogr.,* 2002, **35**, 356.

10 A. Coelho, Topas-Academic, *4.1*, Coelho Software, Australia 2007.

11 J. Bergmann, R. Kleeberg, A. Haase, B. Breidenstein, *Mater. Sci. Forum*, 2000, **347-349**, 303.

12 R. W. Cheary, A. Coelho, J. P. Cline, *J. Res. Natl. Inst. Stand. Technol*., 2004, **109**, 1.

13 J. M. Jarvinen, *J. Appl. Crystallogr.*, 1993, **26**, 525.

14 S. J. Sedlmaier, M. Eberspächer, W. Schnick, *Z. Anorg. Allg. Chem.*, 2010, **637**, 362.

15 A. Marchuk, V. Celinski, J. Schmedt auf der Günne, W. Schnick, *Chem. Eur. J.,* 2015, **21**, 5836.

16 A. S. Wills, *VaList, version 4.0.7*, University College London, UK, 2010.